Univerza v Ljubljani

Institut "Jožef Stefan" , Ljubljana

61 111 Ljubljana, Jamova 39, pp 100 / Tel : 61 12 59 199 / Fax : 61 12 57 074, 61 12 61 029

IJS Report
IJS - DP -
December 1997

Beam test of a full system prototype of the HERA-B RICH

S. Korpar[a,b], M. Starič[a], D. Škrk[a] and P. Križan[c,a]

[a] *"J. Stefan" Institute, Ljubljana, Slovenia,*

[b] *Faculty of Chemistry and Chemical Engineering, University of Maribor, Slovenia, ,*

[c] *Faculty of Mathematics and Physics, University of Ljubljana, Slovenia*

DRAFT DRAFT DRAFT DRAFT DRAFT DRAFT DRAFT DRAFT

Abstract

We report on the results of a beam test of the HERA-B RICH supermodule prototype with the complete light collection system, as carried out in November 1997.

1 Apparatus

In the present beam test we have used the usual RICH set-up which was in previous years employed to test the three sorts of photon detectors for the HERA-B RICH. The same photon detector supermodule prototype was used as in the summer 1997 tests in the HERA-B area. The following changes were made:

- the final CAEN high voltage system was used, with four high voltage channels
- PMT's employed were organized according to the optimum high voltage, as determined from the quality assessment tests

The part of the photon detector, relevant to the exit window of the radiator vessel was equipped with PMTs as shown in Fig. 1. The subdivision between M4 and M16 tubes remained the same as in the previous supermodule tests to make use of the existing cabling, and was clearly not optimal for the present measurement. Note that the supermodule is positioned with its longer side horizontally, i.e. it extends to the left and to the right from the region shown.

The M4 and M16 tubes were chosen by requiring their optimal high voltage to be within an interval of 30 V and 15 V, respectively.

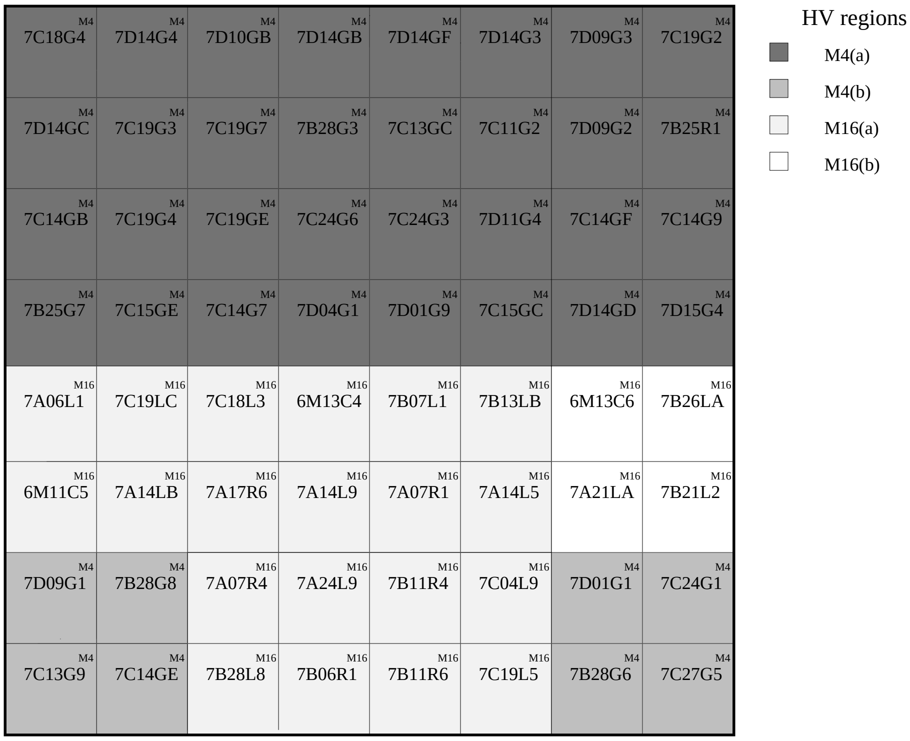

Figure 1: *The equipment of the sensitive surface: PMT type and serial number. The groups of PMTs with a common high voltage supply channel are indicated in grey scale.*

The digital signals from ASD8 chips were led to the FED boards, which, in turn, were read-out by a sharc board. Tracking chambers (i.e. TDCs of the delay line read-out) were added to the DAQ system. The system behaved stably, as was also the case in our previous studies, with an exception of one of the M16 ASD8 boards, which oscillated, most probably due to imperfect grounding (c.f. Figs. 4, 10). Again, the problem of the present version of FED showed up in form of missing data from some ASD8 boards (e.g. in Figs. 10).

The radiator vessel volume (2 m^3) was filled with C_4F_{10} in spring, and was left closed since then. The present concentration of C_4F_{10} amounts to 37%, and was estimated from the measured value of the Čerenkov ring radius (Fig. 2), from which a Čerenkov angle of 37 mradian is deduced. Note that the final C_4F_{10} concentration in the spring test was 66%.

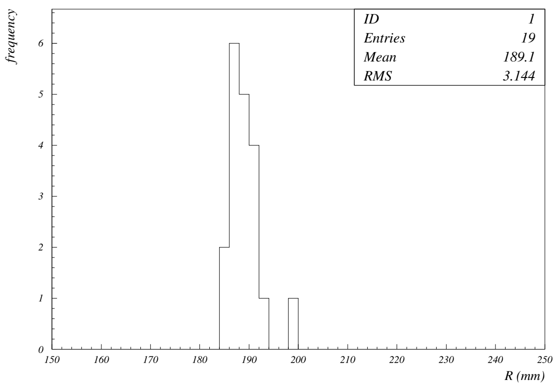

Figure 2: *Ring radius as extracted from various runs with different ring positions.*

2 High voltage scan

To check the high voltage setting, a high voltage scan was carried out, and each group of tubes was separately analyzed.

From the two sets of measurements (Fig. 3) we chose the HV value of 750 V for the M16 PMT's, and 800 V for M4's.

3 Measurements

The following measurements were performed:

- with bare PMTs attached to the vessel,
- with the plexi-glass window,
- with the lens system, and

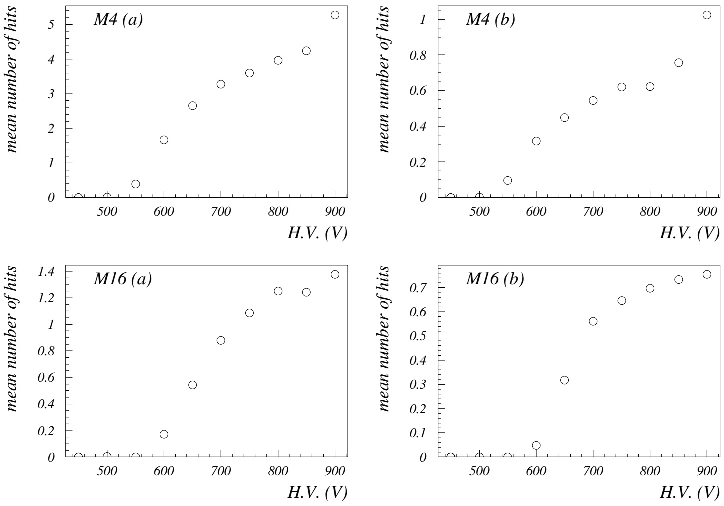

Figure 3: *Number of hits per event per PMT group (Fig. 1) shown as a function of the high voltage.*

- with both the plexi-glass and lenses.

To study various background sources, measurements were made

- without high voltage applied to the PMTs,
- with various pipelines.

The information on the runs is collected in the table below. The raw data can be found on the ftp directory, where they are supplemented by a sample routine for decoding, and a run log, all summarized in the README file.

BEAM TEST RUNS DATA 11/97						
	high voltage (V)				number	
file	M4(a)	M4(b)	M16(a)	M16(b)	of events	comment
high voltage scan						
run_57.dat	450	450	450	450	10000	
run_59.dat	500	500	500	500	10000	
run_60.dat	550	550	550	550	10000	
run_61.dat	600	600	600	600	10000	
run_62.dat	650	650	650	650	10000	
run_63.dat	700	700	700	700	10000	
run_64.dat	750	750	750	750	10000	
run_65.dat	800	800	800	800	10000	
run_66.dat	850	850	850	850	10000	
run_67.dat	900	900	900	900	10000	
background measurements						
run_68.dat	0	0	0	0	10000	
run_69.dat	0	0	0	0	50000	
measurements without lens system and without plexi glass window						
run_70.dat	750	750	800	800	10000	
run_71.dat	750	750	800	800	20000	
measurements without lens system and with plexi glass window						
run_73.dat	750	750	800	800	10000	
run_74.dat	750	750	800	800	20000	
run_75.dat	750	750	800	800	20000	
measurements with lens system and with plexi glass window						
run_76.dat	750	750	800	800	5000	light leak
run_77.dat	750	750	800	800	10000	light leak
run_78.dat	750	750	800	800	10000	light leak
run_79.dat	750	750	800	800	11600	light leak
run_80.dat	750	750	800	800	16320	light leak
run_81.dat	750	750	800	800	15040	light leak
run_82.dat	750	750	800	800	20000	
run_83.dat	750	750	800	800	20000	
run_84.dat	750	750	800	800	20000	
run_85.dat	750	750	800	800	20000	mirror: R: + 1 0/8
run_86.dat	750	750	800	800	18300	mirror: R: + 2 0/8
run_87.dat	750	750	800	800	20000	mirror: R: - 1 0/8
measurements with lens system and without plexi glass window						
run_93.dat	750	750	800	800	10000	pipeline 0
run_94.dat	750	750	800	800	10000	pipeline 1
run_95.dat	750	750	800	800	8240	pipeline 4
run_96.dat	750	750	800	800	8400	pipeline 8
run_97.dat	750	750	800	800	20000	pipeline 0
run_98.dat	750	750	800	800	20000	mirror: R: + 1 0/8
run_99.dat	750	750	800	800	16880	mirror: R: + 2 0/8
run_100.dat	750	750	800	800	20000	mirror: R: - 1 0/8

For each measurement, the raw data were analyzed in the following way. The Čerenkov ring radius and the number of hits were determined from the distribution of measured hits over ring radius (Figs. 7-10). The number of observed hits was normalized to the full ring and full detector coverage. The resolution of the counter was determined by first correcting the hit coordinates with tracker information on an event by event basis.

The analysis was carried out parallel to the tests, which not only sped up the measurement, but also allowed for a fast feed-back. By looking at the data of runs 76-81 a light leak was observed (Fig. 4) and repaired.

4 Backgrounds

Several contributions to the background were studied. As the first, we have recorded data without HV on the PMTs. Less than 0.01 background hits were observed per event (a 1 μs long interval).

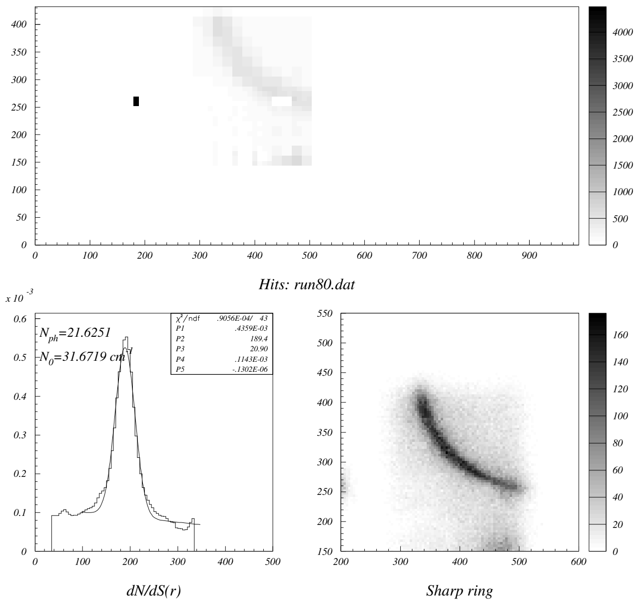

Figure 4: *Run 80: data taken with a light leak below the ring. To the left two oscillating channels of an ASD8 board can be seen.*

Consecutive pipelines were investigated as well. While in the proper pipeline step (0) we observe 9.7 hits per event, in pipe 4 and 8 there are only 0.5. From this value we estimate a background rate of 3 kHz per M4 pads and 1 kHz per M16 pads.

The dominant background contribution is, however, related to the electron beam. This becomes evident if we plot in the same figure the hit distribution over ring radius for four different ring positions (Fig. 5). Note that such a background distribution was also observed with other photon detectors in the same set-up, and is related to the start of an electron shower. The background level is, of course, correlated to the amount of material in the beam in the upstream test zone (e.g. a much lower level was observed in the spring beam test [1] when no experimet was mounted upstream).

5 Resolution in the Čerenkov angle

The resolution in Čerenkov angle is expected to be dominated by the following contributions:

- detector granularity (dominated by M4) $\sigma_{msc} = \frac{18}{5000\sqrt{12}} = 1.0$ mradian
- multiple scattering of electrons, $\sigma_{msc} = \frac{2}{3}\frac{15MeV/c}{p}\sqrt{\frac{l}{X_0}} = 0.9$ mradian
- cromatic aberration $\sigma_{cr} \approx 0.3$ mradian

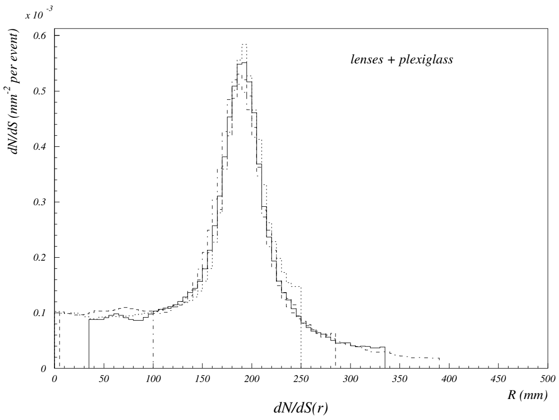

Figure 5: *Runs 84-87: hit distribution over Čerenkov ring radius for four different ring positions.*

- tracking system resolution $\sigma_{tr} \approx 0.2$ mradian

If summed in quadrature, the resulting expected resolution is 1.4 mradian. The observed sigma (Fig. 6), 2 mradian, is clearly larger, and the discrepancy is under study.

6 Number of detected photons

In the first estimate we have fitted the distribution over raw hit radius (Figs. 7-10) with a sum of a Gaussian and linear function. The distribution is plotted as the hit surface density, normalized to the full ring coverage. Specifically, the dead channels because of the error in the FED were excluded from the acceptance. The results of the fit are indicated in each of the Figs. 7-10.

To estimate one of the possible systematic errors, measurements were carried out with the spherical mirror tilted by different angles (as e.g. in Fig. refrun100), and the data were analyzed in the same way. For the full system (lenses and plexi glass) four different ring positions were analyzed (runs 84-87). The corresponding numbers of photons per ring are 29.6, 28.6, 30.7 and 29.2. This, in turn, tells us that none of the measurements is by more than 3% away from the average value, 29.5.

To study the influence of the parametrisation of the background below the Čerenkov peak on the number of detected photons, we have assumed it follows a linear function, fixed the starting point (to a ring radius of 100 mm in Fig. 5), and varied the end point of the line.

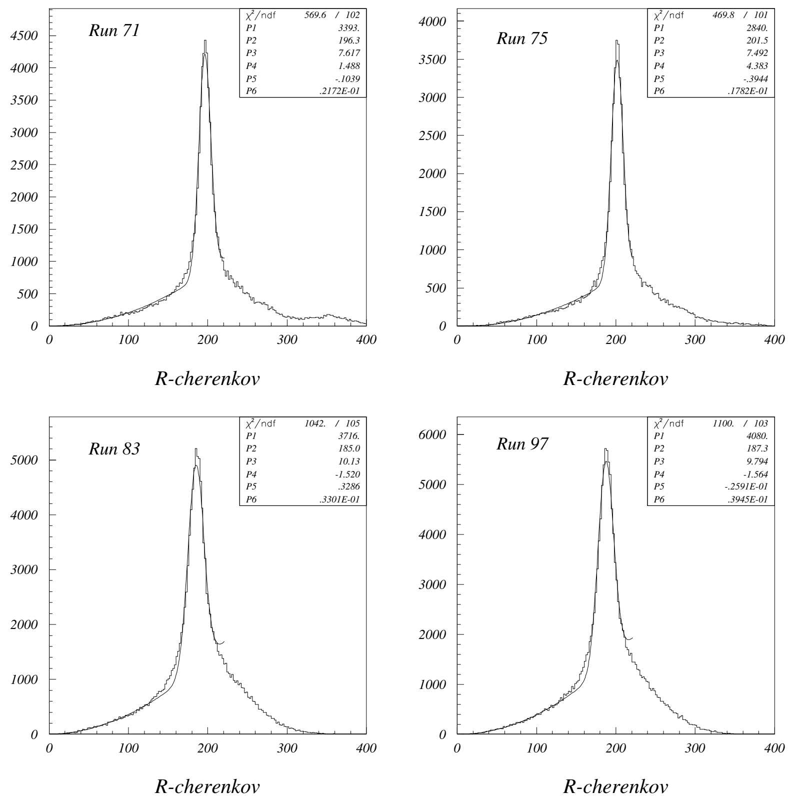

Figure 6: *Distribution of hits, corrected with tracking system information, for typical runs with the lens system (bottom) and without it (top). The distributions were fitted by a sum of Gaussian and quadratic functions.*

End point of the line at ring radius (Fig. 5)	number of photons
370 mm	30.1
295 mm	29.5
285 mm	29.5
275 mm	28.8
260 mm	27.7
240 mm	24.8

To estimate the error due to parametrisation of background, we use the first five values to arrive at a sigma of 3%. The last estimate essentially assumes that the background under the peak is constant, and equal to the value at smaller ring radii. This is clearly a very conservative assumption, and we shall quote the corresponding value for each measurement as N_{ph}^{min}.

The results of measurements with various set-ups are summarized in the table below.

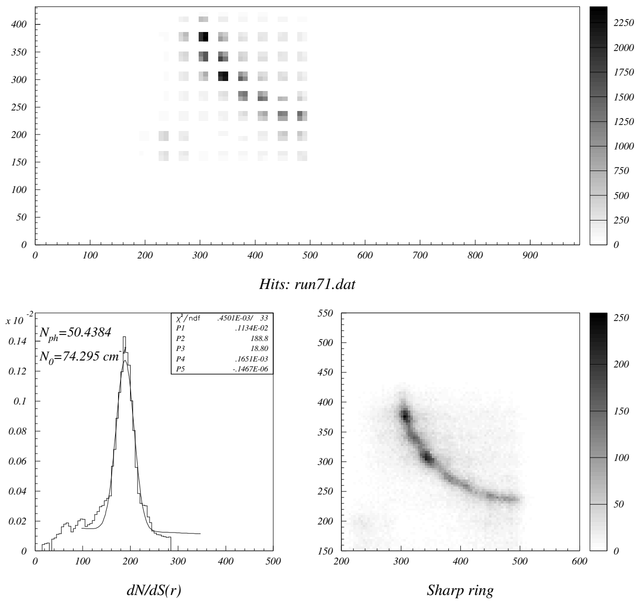

Figure 7: *Run 71: bare PMTs, raw accumulated data, hit coordinates corrected with tracker information and the distribution over the raw Čerenkov angle, with results of fit indicated.*

Set-up	N_{ph}	N_{ph}^{min}
Bare tubes	17.2	14.9
Plexi-glass	12.4	11.5
Lenses	33.2	28.3
Lenses, plexi	29.6	25.5

From the number of photons deduced in this way we can calculate the efficiency of the light collection system, by assuming a 0.25 active surface of the bare PMTs. The results are summarized in the table below.

Component	Transmission, M16	calculated M4	Transmission, measured
Lenses (for PMTs with plexi)	0.63	0.60	0.56
Plexi-glass (for PMTs with lenses)	0.92	0.91	0.89
Plexi-glass alone	0.89	0.70	0.78 (dominated by M4)
Lenses alone	0.60	0.46	0.48 (dominated by M4)
Lenses and plexi-glass	0.55	0.42	0.43 (dominated by M4)

Since the M4 PMTs are sensitive in UV as well, and the ring position was such that it is dominated by the M4 response, the present measurement only gives average values of

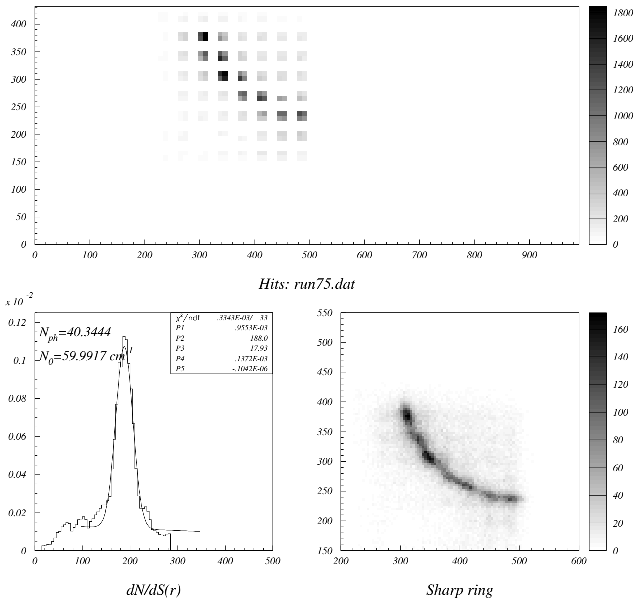

Figure 8: *Run 75: PMTs with plexi-glass window, raw accumulated data, hit coordinates corrected with tracker information and the distribution over the raw Čerenkov angle, with results of fit indicated.*

the stand-alone transmission of the plexi-glass, lenses, or lenses combined with plexi-glass, which are very much weighted towards the M4s.

7 Figure of merit N_0

The figure of merit N_0 of the tested RICH counter was extracted from the measured number of photons per ring by taking into account that

$$N_0 = \frac{N_{ph}}{\theta_c^2 l},$$

where l is the radiator length (5 m). The Čerenkov angle is determined from the average ring radius (Fig. 2), and amounts to $37.3(1 \pm 0.017)$ mradian. The resulting values are listed in the table below. Again, the estimate based on a very conservative assumption on the background form is used to derive a the conservative value of N_0^{min}.

Set-up	N_0	N_0^{min}
Bare tubes	96.2	83.5
Plexi-glass	75.2	64.6
Lenses	47.1	40.2
Lenses, plexi	42.0	35.5

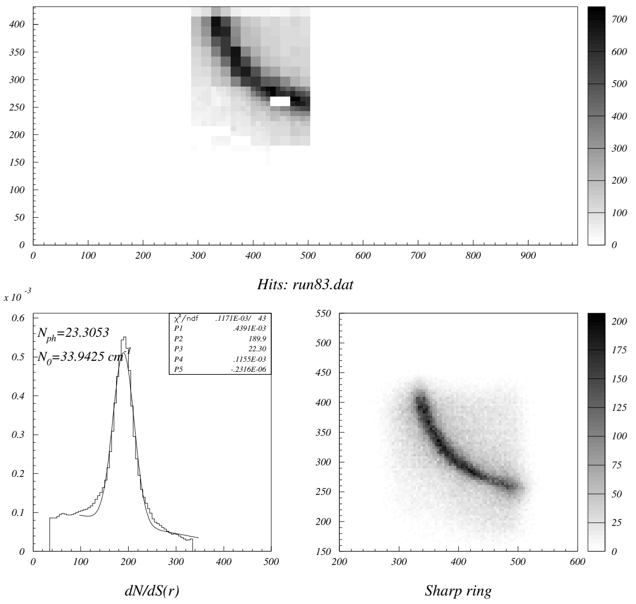

Figure 9: *Run 83: PMTs with lenses, raw accumulated data, hit coordinates corrected with tracker information and the distribution over the raw Čerenkov angle, with results of fit indicated.*

We note, however, that the ring radius could only be determined with a limited accuracy because only about a fifth of the ring was detected on the photon detector. The resulting error was estimated from the distribution of fitted radii (Fig. 2) to be 3mm R.M.S., corresponding to a 1.5% error in the radius, and a 3% error in N_0.

Clearly, the most relevant number is the figure of merit for the full system,

$$N_0 = (42 \pm 2)\ \mathrm{cm}^{-1},$$

where we have taken into account the three main sources of the error, the parametrisation of background, the dependence of the result on the ring position, and the error in ring radius. To estimate the figure of merit for the HERA-B case, we note that there is an additional mirror if compared to the test set-up, and no quartz window. Also, the spherical mirror used in the set-up is expected to be somewhat inferior to the HERA-B spherical mirrors. Note also that the transmission of quartz is somewhat better than the reflectivity of the mirrors. Without a better information available, it is therefore reasonable to assume that both effects roughly cancel, and the figure of merit remains the same for the HERA-B case. The final value of N_0, 42 cm^{-1}, can then be used to determine the number of photons in the case of HERA-B RICH, where the radiator is shorter ($L = 2.8$ m), and the average Čerenkov angle is expected [2] to be equal to 52 mradian. The expected number of detected Čerenkov photons is thus

$$N_c = N_0 L \theta_c^2 = 32 \pm 2.$$

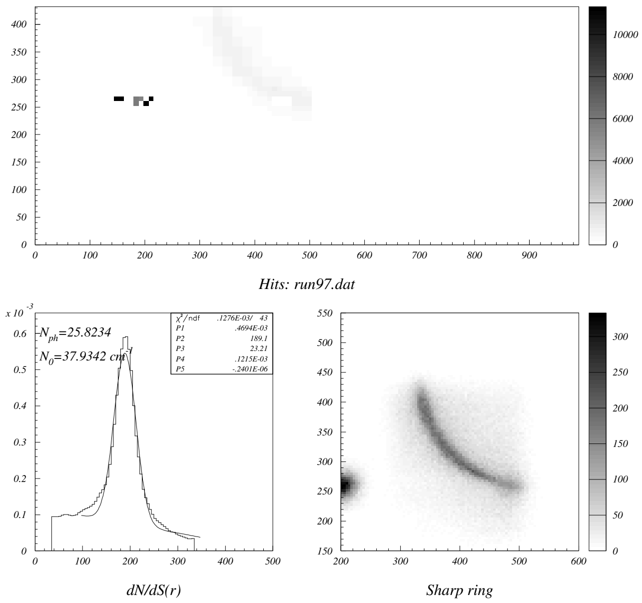

Figure 10: *Run 97: PMTs with plexi-glass window and lenses, raw accumulated data, hit coordinates corrected with tracker information and the distribution over the raw Čerenkov angle, with results of fit indicated.*

References

[1] S. Korpar, R. Pestotnik and P. Križan, Beam test of a RICH with C_4F_{10} gas as radiator and an array of MA-PMTs for photon detection, IJS-DP-7673.

[2] Fokitis et. al., Nucl. Phys. Proc. Suppl., B44 (1995) 246-251.

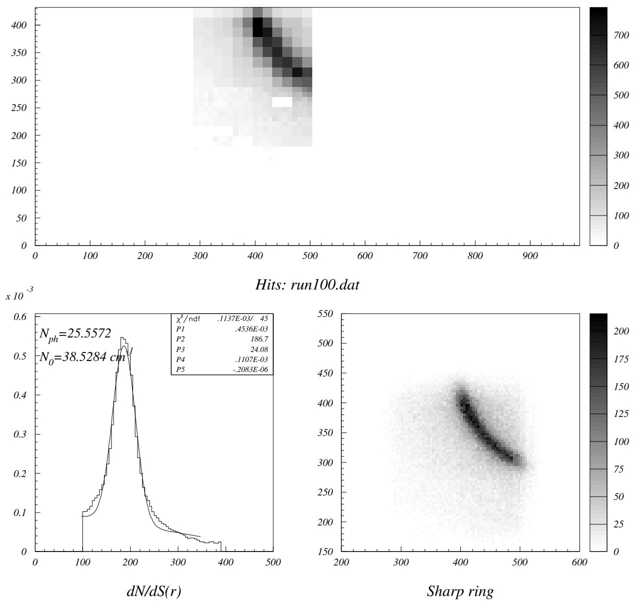

Figure 11: *Run 100: same as 97, but with tilted mirror.*